Electronic Supplementary Material (ESI) for Nanoscale.
This journal is © The Royal Society of Chemistry 2018

# Supporting Information

## Section 1. Particle radius of the SERS-active substrate

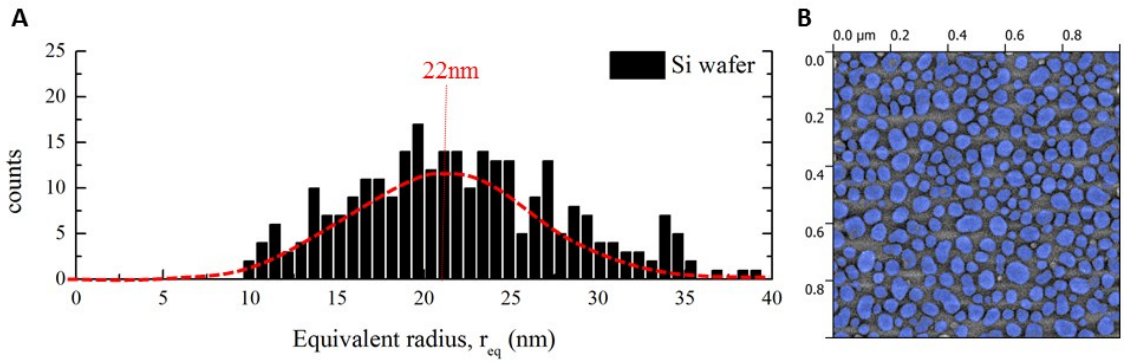


**Figure S1.** (A) Histogram of the silver particle radius distribution for a SERS-active substrate shown in (B). The radii were extracted from the evaluation of each of the particle area (blue) evaluated from the SEM image (B).

## Section 2. Numerical simulation of the refractive index

The refractive index of the substrate has to be taken into account for an accurate description of the electric field enhancement of silver particles on a silicon substrate as a function of the wavelength. This is not straightforward due to the systematic formation of an amorphous silicon oxide layer of unknown nature (and thickness) at the air/silicon interface that is in direct contact with the silver particle.[1, 2] Assuming that the electric field penetrates several nm in the underlying silicon substrate, its presence is detrimental to our ability to extract a clear analytical value.

Figure S2 schematically shows the method used to overcome this challenge. The sum of all refractive indices are unknown and are referred to as an "effective" refractive index at the particle/surface interface as shown in Figure S2A. A "gap distance" is introduced as a parameter representing a distance between the particle and the pure silicon substrate underneath (see the schematic representation in Figure S2B) to account for this unknown parameter. The gap distance is optimized such that the best match with the experimental dark field spectroscopy results is achieved. A summary of the far-field spectral simulations for different gap distances with 1 nm steps is given in Figure S3. Throughout the manuscript, a value of 2 nm has been selected and was systematically applied to the

calculation procedure and always led to simulated spectra that matched the far-field experimental results (except in the context of TERS tip, where the gap of 2 nm was used without experimental comparison due to the difficulties obtaining the actual near-field spectra as pointed out in the main text).

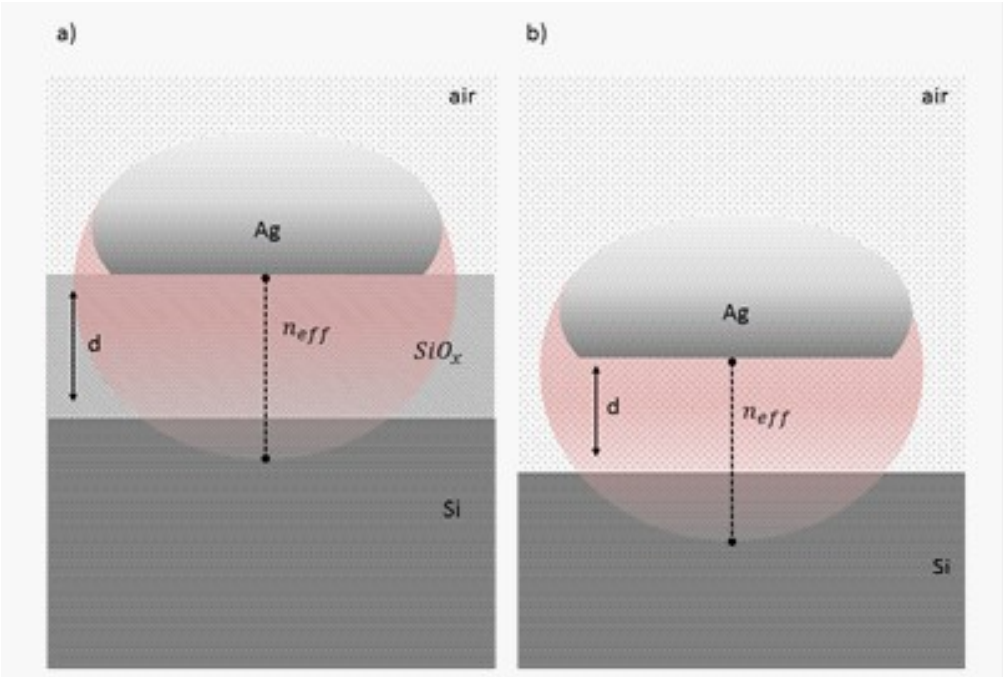


**Figure S2.** Schematic representation of a silver particle deposited on a "silicon" substrate and realistically in direct contact with an amorphous silicon oxide layer. **A)** The electric field penetrates a zone of unknown "effective" refraction index of unknown thickness. **B)** An approximation can be realized by simulating a gap distance between the particle and the pure silicon substrate.

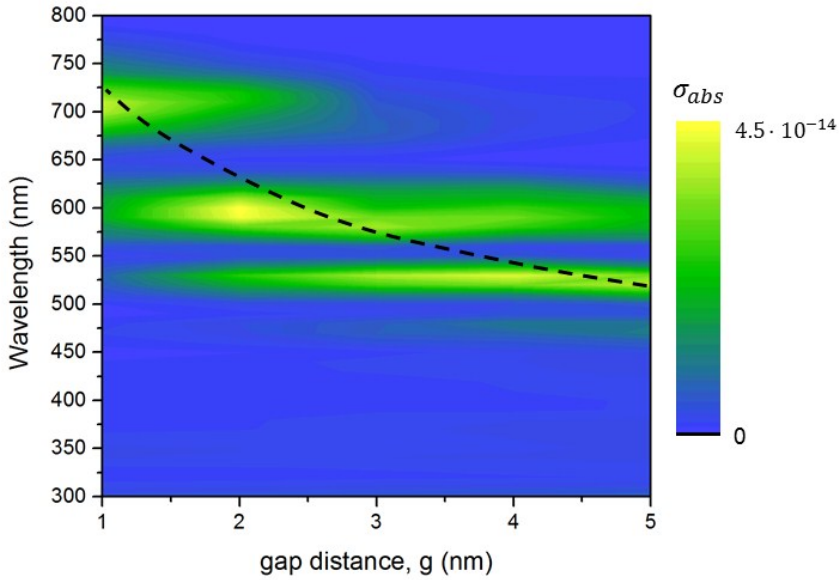


**Figure S3.** Far-field spectra (y axis) from a silver particle film deposited on silicon wafer for several potential gap distances (step size: 1 nm). The gap distance g = 2 nm leads to 3 bands in the simulated spectrum which is consistent with the experimental dark field spectra.

## Section 3. Formalism of the FEM calculation

The 3D FEM model was built in Comsol Multiphysics 4.4 (v.248), using the wave optics module for electromagnetic waves. This module enables calculating the full electric field E, under stationary conditions:

$$\nabla \times \frac{1}{\mu_r}(\nabla \times E) - k_0^2\left(\epsilon_r - \frac{i\sigma}{\omega\epsilon_0}\right)E = 0$$

where $\epsilon$ is the permittivity, $\sigma$ the conductivity, $\mu_r$ the relative permeability, $\omega$ the angular frequency and k the wave vector.

By using the constitutive relation for linear materials ($\sigma = 0, \mu_r = 1$) the formula can be simplified to the Helmholtz equation:

$$\nabla^2 E - k_0^2 \epsilon_r E = 0,$$

which is used in our FEM implementation.

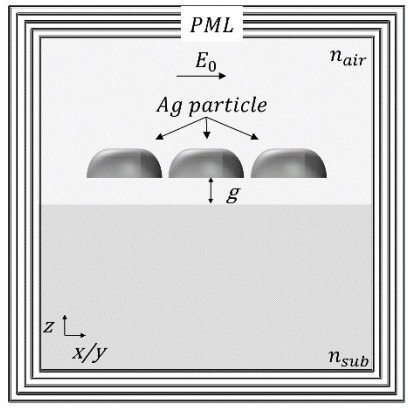


**Figure S4.** Sketch of the numerical boundary layer system with an incident field $E_0$ and a gap distance g between the silver particle and the silicon substrate.

The incident power (P) for the bottom port was calculated according to:

$P = I_0 w^2 \cos(\phi)$

with the incident intensity ($I_0$) set to $E_{ev} = 1V/m$ at the air/substrate interface according to:

$$I_0 = \frac{E_0^2 \cdot n_{air} \cdot c_0 \epsilon_0}{2}$$

where $E_0$ is the incident field, $c_0$ is the speed of light in vacuum and $\epsilon_0$ the vacuum permittivity.

The minimum tetrahedral element mesh size was 9.6 nm around the nanoparticle.

Finally, the stationary direct solver (MUMPS) was used to solve the system of equations. It proved to be effective and numerically robust for this implementation of our model system.

**Section 4. Reproducibility of the far field experimental and simulated spectra**

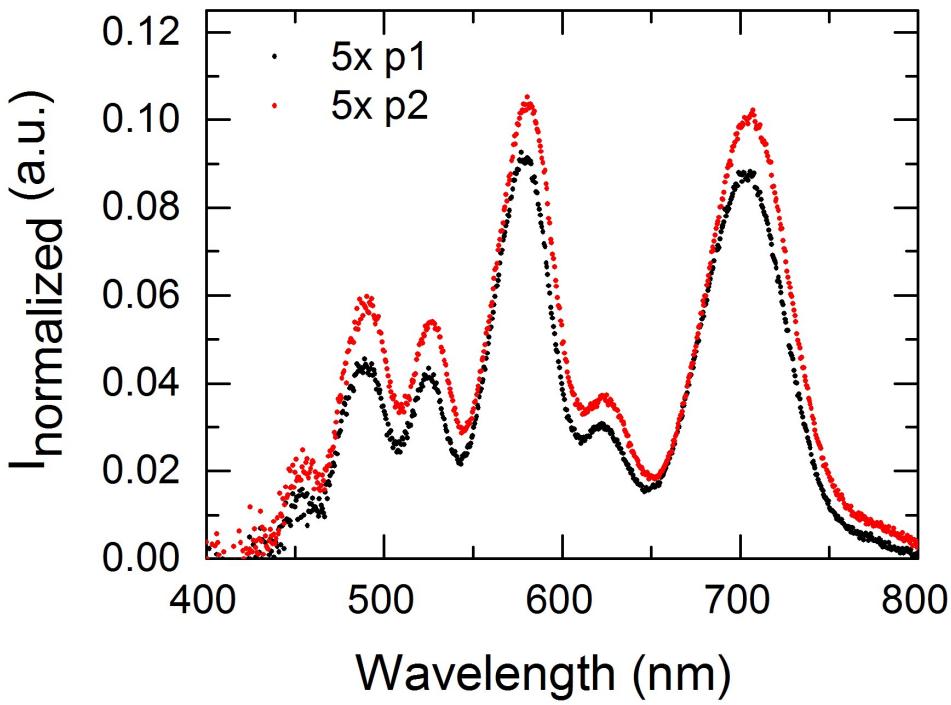


**Figure S5.** Far-field spectra measured by dark field spectroscopy with use of a 5X objective on a SERS-active substrate. The black spectra is copied from Figure 1C (main manuscript) while the red spectra is a different measurement on a second section of the same sample.

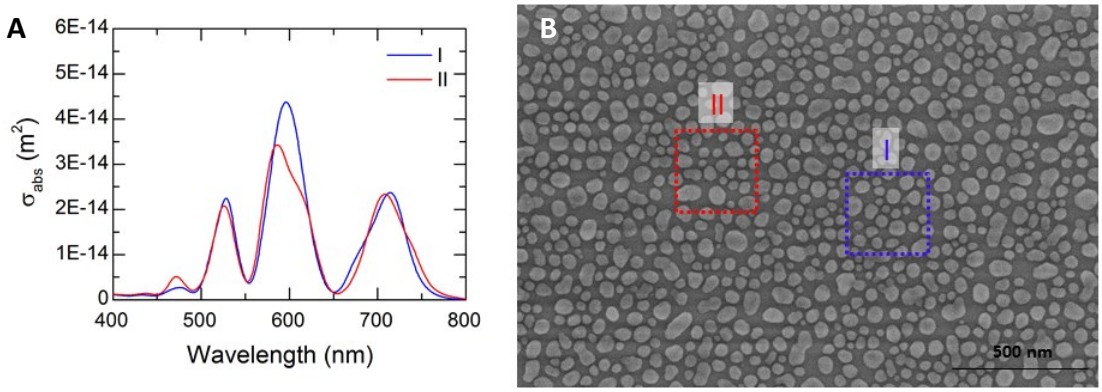


**Figure S6. A)** Far-field spectra calculated from the two distinct parametrized regions identified on the SEM picture shown in **B)**.

## Section 5. Particle radius of the TERS-active tips

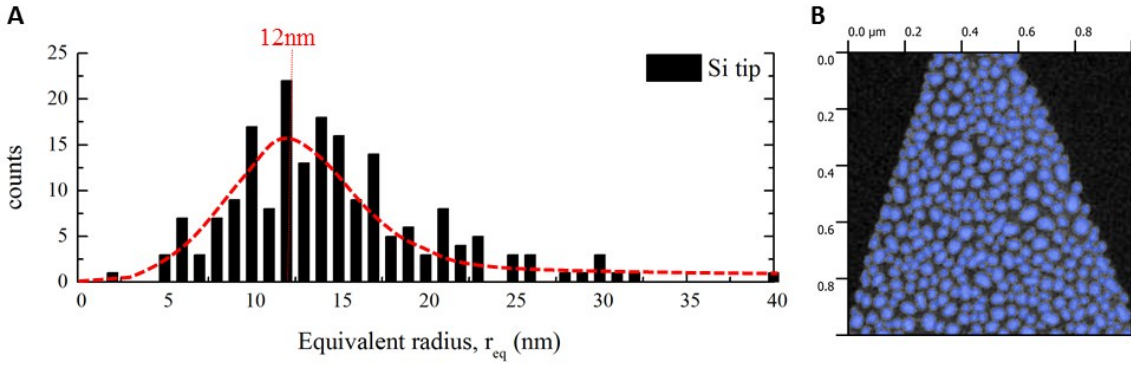


**Figure S7. A)** Histogram of silver particle radius distribution for a TERS-active tip. The radius has been extracted from the evaluation of each of the particle area (blue) evaluated from the SEM image **(B)**

## Section 6. Investigation of the influence of coupling modes on the near field

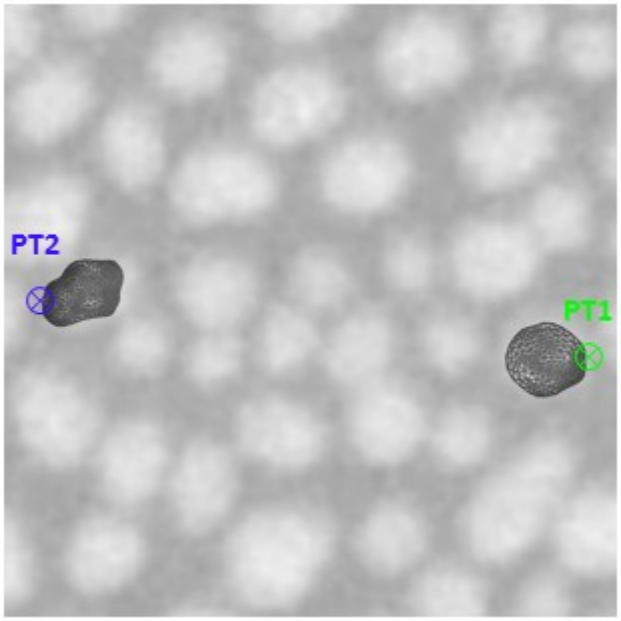


**Figure S8.** Parametrized surface of the TERS-active tip presented in Figure 4B. All particles except the ones close to the selected positions PT1* and PT2* (used for near - field simulation) were eliminated. Consequently, the resulting spectra should be influenced solely by single dipole resonances.

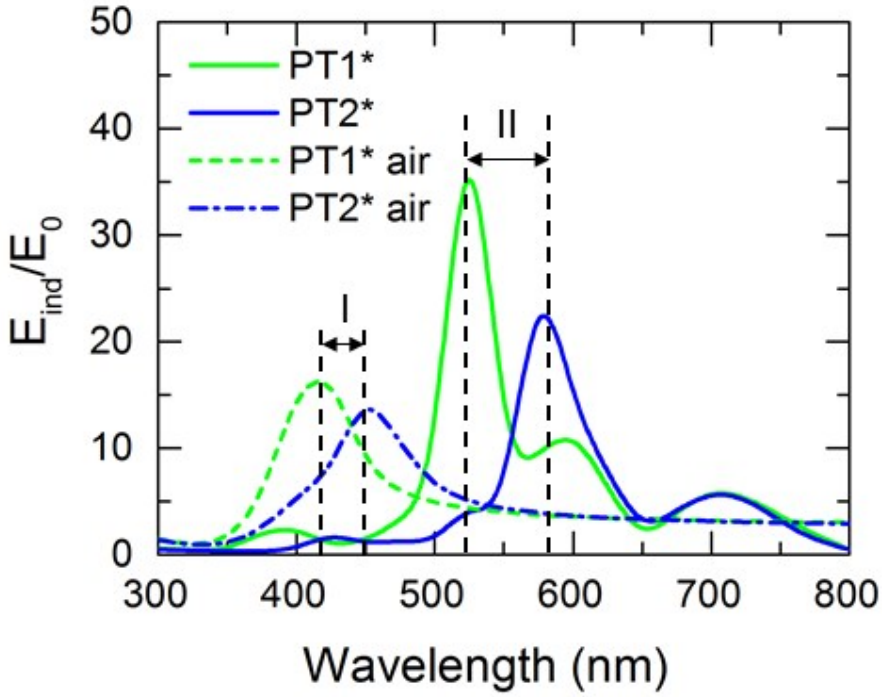


**Figure S9.** Simulation of the near-field spectra for the point location PT1 (green) and PT2 (blue) indicated in figure S8. The full curves are associated to the isolated particle on a silicon substrate (see main text). The dashed curved have been simulated using a gap distance of 50 nm (see section S2) to mimic the behavior of the particle in air, i.e. without the presence of the silicon substrate.

**Section 7. Dark field spectroscopy setup.**

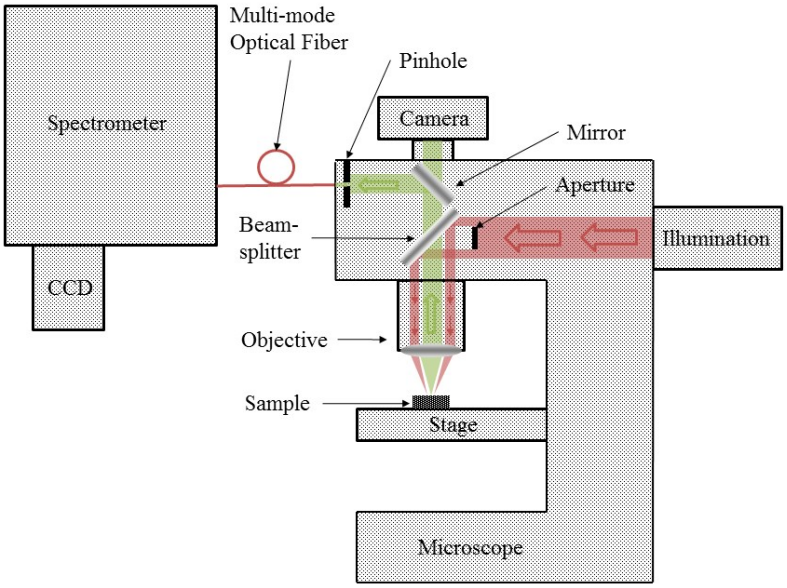


**Figure S10.** Scheme of the dark field microscopy setup in upright illumination mode.

**References.**


1. M. Morita, T. Ohmi, E. Hasegawa, M. Kawakami and K. Suma, *Applied Physics Letters*, 1989, **55**, 562-564.
2. M. J. Kim and R. W. Carpenter, *Journal of Materials Research*, 2011, **5**, 347-351.